

Research on Remote Sensing Applications in Malta

Massimo Darmanin

Institute of Information & Communication Technology

Malta College of Arts, Science & Technology

Corradino Hill

Paola PLA 9032

massimo.darmanin.c10229@mcast.edu.mt

Abstract—This research explores the possibility of detecting, observing and analysing the Urban Heat Island(UHI) effect over the Maltese islands. The focus of this study was based on the collection of data gathered through remote sensing technologies for the months of March till August of the years 2019, 2020 and 2021. The inclusion of March, April and May came from the idea of observing what happened during the lockdown Malta had experienced during these months of the year 2020. Sentinel-3 remotely sensed data was utilised to conduct research for this project. This study produced the Land Surface Temperature(LST) and Normalised Difference Vegetation Index(NDVI) by reprojecting, cloud masking and excluding high LST Uncertainty pixel values via the products obtained from Sentinel-3 using ESA's common architecture for all Sentinel Toolboxes, Snap Desktop. Study areas included the Maltese islands, the main island of Malta and its urban and rural areas. This was achieved by using the contouring option in QGIS which this research was able to focus its area of study to specific parts of Malta. Hence, NDVI was used to look into any possible links between urban and rural LST of Malta. Observations revealed that the UHI effect during summer were more intense than winter, however the predicted shape and usual observations usually associated with inland cities UHI effects were not present. Instead, the UHI in Winter, albeit much less intense, behaves much more like the observations in literature reviewed. These unique observations have been associated with coastal cities. The effect of the sea breeze on temperatures is mitigated by the presence of vast bodies of water, causing local climate change. These observations were backed by that data analysis of each product, which was then split into 2 time periods; Covid period (March, April and May) and Summer period (June, July and August). Each period was composed of multiple products, within the months mentioned, for the years of 2019 till 2021. Analysed data showed an upward trend in LST values and downward trend for NDVI, slowing down in momentum briefly in the year 2020. Moreover, this research looked into the possibility of observing LST and NDVI correlation, which was observed and calculated its correlation coefficient.

Index Terms—UHI, Remote Sensing, LST, NDVI, Urban area, Rural area, Climate, Coastal City

I. INTRODUCTION

Technology has progressed since the humble beginnings of the tiny satellite resurgence in the 1980s to support an ever more accurate sensory readout and data delivered. Prior to the recent economic boom that Malta has seen in the previous years, its leaders rarely saw the need to investigate the possible applications of remote sensing the way bigger, more affluent countries do. Despite the fact that Malta is a small island, with a recent shift in the economy and a diversification of influence

from international investments, there is an ever-increasing need to keep up with and extend prospective applications fit for accurately monitoring and surveilling its area.

A. Motivation

This paper tries to propose a solution to the problem by presenting data and a case study of how remote sensing can help this island. Prior to the Sentinel Missions, publicly available remote sensing satellites were not accurate or precise enough for Malta to be considered a feasible choice. A growing problem currently being faced by the Maltese citizens is the ever encroachment of development in rural areas and the lack of green spaces in the urbanised areas when compared to other foreign countries such as Slovenia, Sweden or Switzerland. Obviously these countries do not suffer from the same constraints our little island has to face. However, by using remote sensing technologies, our limited resources can be used to their utmost potential, building a better planned future while mitigating and reducing our footprint on the environment and our own health.

B. Aim

The main goal of this research is about using readily available remote sensing technologies and find a use case to study and observe over the Maltese Islands. By doing so, this research hopes to look at all the challenges faced throughout the study in order to document, observe and analyse. The Maltese Islands' population growth and economic development have resulted in a rise in the demand for housing and other amenities. These and other causes contributed to the phenomena of urban sprawl, particularly in rural areas. For this reason, UHI (Urban Heat Island effect) has been chosen to be studied and observed. The reason behind observing and analysing UHI instead of other case studies is due to the fact that there is very limited material and awareness on the subject in Malta. Therefore this research's aim is about exploring remote-sensing technologies and how they may benefit our society while also raising awareness about UHI and its impact on society while exploring the possibility of finding any correlation between LST (Land Surface Temperature) and NDVI (Normalised Difference Vegetation Index).

C. Is Remote Sensing a viable option to track and observe the UHI effect in Malta?

Is remote sensing for Malta a viable option? What remote sensing applications are best suited for Malta? Are these choices dependable? This research will focus on the data extraction and manipulation deriving from remote sensing products, more specifically, the SLSTR Level-2 LST products from the Sentinel-3 mission. By answering this question, this research hopes to shed more insights on the use cases available which can be done using current remote sensing technologies and their ability to cater to the Maltese geographical situation.

D. Does the UHI effect exist in Malta?

Does UHI exist in Malta? And if it does exist, to what level does the UHI effect the Maltese landscape? Is it limited to a single area? Does it envelope the whole islands or is it specific to the individual area? What factors are driving the UHI effect?

E. Can UHI be tracked and analysed accurately over a period of years using Remote Sensing technologies?

If the UHI effect exists in Malta, is it a viable option to use remote sensing products in order to track and analyse this phenom over a period of years? Is the data being used reliable and accurate? Are there any external factors to look into when using remote sensing products for such a case study?

F. What kind of observations can this data provide?

What kind of data does remote sensing products offer? Can this data be manipulated with other metrics or indexes in order to produce extra relevant data? What are the limitations of this data? What can we learn as a society from the observations produced and analysed?

II. LITERATURE REVIEW

A. The Urban Area

Urban areas, also referred to as built-up areas, are human settlements with high population densities and infrastructures of the built areas. Urbanisation creates urban areas, and these are usually categorised by the urban morphology such as cities, towns or suburbs. Five key parameters were used in the UNICEF report of 2021¹ to characterise an urban area: administrative criteria or political boundaries, the existence of urban characteristics, economic drive, population density and a threshold population size [1]. The threshold population size for an urban settlement is generally around 2,000 residents, however, this number varies from 200 to 50,000 people². This means that the figure which defines an urban area may differ from one place to another.

¹<https://www.unicef.org/media/84881/file/SOWC-2012-executive-summary.pdf>

²<https://ourworldindata.org/urbanization>

B. Urban Sprawl

The first recorded word “sprawl” was used by Earle Draper, who was one of the earliest city planners in the South Eastern side of the United States of America in the late 1930s [2]. However, the phrase “urban sprawl” has been defined in many different ways. According to [3], this is due to the fact that Urban sprawling is a phenomenon which can be viewed from different perspectives. As a result, the definition of urban sprawl is very ambiguous, which is why researchers opt for solely discussing term without applying their own definition [3].

C. Study Area

Malta is an archipelago in the centre area of the Mediterranean sea, about 80km south of Italy. Only the three largest islands are inhabited. These islands, Malta, Gozo and Comino consist of numerous bays, which feature landscapes of low hills with terraced fields. The islands have a Mediterranean climate, with mild winters and hot summers. Even though Malta has no permanent rivers or lakes due to its climate, it does temporally host some type of water bodies such as valleys and ponds during times of high rainfall. Rainfall generally happens during autumn and winter as summer is mostly dry.

D. Climate

Average yearly temperature is around 23°C during daytime and 15.5°C during nighttime. The coldest month of the year is January with an average temperature of 12.9°C while the warmest month is August, with an average temperature of 27.5°C. Shifts in temperature are rare occurrences for the islands³. The approximate number of sunshine hours is around 3000 per annum, averaging from 5.2 hours in December to 12 hours in July. This is important since on average, Malta has double that of cities in the Northern part of Europe⁴.

E. Urbanisation in Malta

Eurostat describes Malta as being composed of two larger urban areas, which they branded as “Valletta” and “Gozo”. It should be noted that the main urban area covers the entire main island. The European Spatial Planning Observation Network described Malta as a functional urban area (FUA). The Urban sprawl in Malta is always increasing since population growth creates the need for more housing units. According to the⁵, since 1998 the percentage of the Maltese Urban population grew from around 91.7% to just below 95% in 2018 and is increasing each year. ESPON and Eu Commission studies stated that, “the whole territory of Malta constitutes a single urban region”. With a population of around 400,000 residents and an area of 3.16 km², Malta is one of the most densely populated countries around the globe⁶.

³<http://meteo-climat-bzh.dyndns.org/listenormale-1991-2020-1-p138.php>

⁴<https://web.archive.org/web/20150806124550/http://www.maltaweather.com/information/maltas-climate/>

⁵<https://data.worldbank.org/topic/urban-development?end=2018&locations=MT&start=1998>

⁶<https://worldpopulationreview.com/countries/malta-population/>

When comparing urban permeation within the 28 European Union and 4 European Free Trade Association countries, Malta scored a very high urban permeation units per square meter value. So high in fact that when combining the total permeation units per square meter value for the aforementioned countries, the result is three times less than that of the Maltese Islands alone, which was 5.5 urban permeation units per square meter⁷. Another study by [4] shows that 64 countries worldwide surpass the degree of urbanisation and agglomeration, and Malta was one of these countries mentioned.

F. Urban Heat Island (UHI)

Research and studies regarding Urbanisation frequently speak of the Urban Heat Island effect due to the fact that it is the biggest threat associated with urbanisation and industrialism [5]. The Urban Heat Island (UHI) effect, is a heat accumulation phenomenon often characterised by the urban climate created by urban constructions and general human activities [6], [7]. According to [8], Urban Heat Islands have been well studied and documented, however the basic understanding of this topic is very limited. This has changed since further advancements in technology and global warming has been taken into priority in last few years. Starting in the early 19th century, a scholar named Luke Howard, was the first person to measure and discuss the UHI effects, during a study about the urban climate in London, England. Following this research, many scholars worldwide started researching on the characteristics of the UHI effect [9]. These studies observed that there was a significant difference between air temperature recorded at urban areas with those located in rural regions [10]. This affect of urbanisation on long-term temperature records, has also been detected for cities with populations less than 10,000 citizens [11]. A number of key features keep reappearing whenever urban sprawling is mentioned in texts. Most of them mention fragmentation, decentralisation, loss of space and density features [12]. [13] analysed social science and planning literature and suggested that definitions of urban sprawl are to be categorised into six general groups, which are:

- 1) The embodiment of the characteristics of sprawl such as Los Angeles.
- 2) The aesthetic judgement about a general pattern of the urban development.
- 3) The cause of an externality such as the isolation of the poor in the inner city, relying heavily on motor vehicles, destruction and loss of environmental qualities and the spatial discrepancy between jobs and housing.
- 4) The result or effect of an independent variable such as poor planning, fragmentation in the local governance, or exclusionary zoning.
- 5) The existing pattern of development such as distance to central facilities, leapfrogging, dispersion of em-

ployment, residential development and continuous strip development.

- 6) The development of that of which occurs over a period of time as an urban area expands outwards.

The very first studies done by the World Meteorological Organisation (1982) and [8] showed that UHI effect has the potential of increasing air temperature in a city by around 2°C and 8°C. That said, more recent studies using more accurate measurements illustrate an increase in temperature by 5°C and 15°C [14]. UHI stems from the changing nature of our urban cities, the result of a decrease in vegetation, higher prevalence of dark surface and an increase in anthropogenic heat production [15]. [16] conducted a study on different metropolitan areas in the USA and concluded that knowledge of the urban fabric and surface conditions of our cities is an important aspect to look at in order to explore and research further effects of possible UHI mitigation measures.

The Urban Heat Island can be represented by plotting a curve from one side of the urban city to the other, thus mapping graphically the change in temperature from rural to urban environment and then back again to rural. According to [8] the 'Island' part would be represented by a big spike in the middle of the graph, which generally copies the outline of the urban structures within the given area and is bound by the cliffs either side that mark the urban and rural boundary. This way, UHI is easier to spot the increased temperature difference.

The biggest difference in air temperature between urban and rural areas is often observed during the night, with differences in surface radiant temperature at around midday [17]. It was noted that in terms of readings, during the day, rural areas give out a higher LST mean than urban areas, both in periods of heat wave and periods of normal environmental conditions. However, results from data readings during the night showed that rural areas had an average mean LST lower than urban areas, regardless of environmental conditions. The decrease in amount of heat stored in the soil and surface structures covered by transpiring vegetation in rural areas, compared to the relatively unvegetated urban areas, has been cited as a major contributor to the UHI effect [18]. There are a number of academic sources that confirm this situation between rural and urban areas, especially during the early hours in the morning and at night, motivated by the solar radiation received during the day [19]–[23].

However, a study conducted by [24], partially focusing on coastal cities, concluded that sea breezes, which are most prominent around the coast, can reduce temperatures and affect the UHI's configuration. Three of the four weather stations used in this study were located in an area with a maximum distance from the coast of less than 2 km, and hence are subject to the synergistic effect of sea and land wind, as well as the UHI phenomena. This emphasises the importance of taking non-thermometric factors into account, such as elevation, orientation, or position, as well as population expansion and the types of built environment and land cover [25], [26].

⁷<https://www.eea.europa.eu/publications/environmental-indicator-report-2016/download>

G. Effects

As a side effect, Urban Heat Islands release excessive amounts of pollution and greenhouse gases to the atmosphere (EPA, 2020). Children and elderly are prone to extreme temperatures and heatwaves. UHIs have a tendency to multiply the effects of heatwaves. This leads the UHI to influence the air quality in urbanised areas. [27] found that an increase in temperature leads to an increase of chemical reactions that forms ozone. Ozone is a toxic greenhouse gas to humans at ground level. This leads to a range of respiratory ailments such as asthma [28]. This means that heat islands are the downfall of quality of life around the urban areas [5].

H. Satellites, Orbits and Sensors

The 1990s was a decade in which the use of remote sensing exploded in popularity, using satellite images with TIRS (Thermal Infrared Sensors) to avoid and cut economic costs related to in situ measurements and the scale of operations that bring with them large cities. For the past few decades, various satellite programs have been developed to produce LST products such as Sentinel-3, Modis, EcoStress, Ladis, LandSat8 and various others. The most recent being EcoStress, which was launched into orbit and docked to the ISS (International Space Station) in 2018, Sentinel-3, which comprises of 3 satellite constellation, having the first two satellites launched in 2016 and 2018 respectively, while LandSat 8 launched in 2013. EcoStress, having five TIRS bands and a single shortwave infrared band, provides with LST estimates at a resolution of 70m. Sentinel-3 comes equipped with three TIRS channels, S7-S9 bands, which provide LST estimates with a resolution of 1km. Interestingly, although being the longest in orbit, LandSat 8 features two TIRS bands 10 and 11 which provide LST estimates at a resolution of 100m.

I. Land cover classification

Land use classification can be obtained by using data acquired from remote sensing products and process the data by means of image classification. Image classification is the manipulation remote sensing data by applying a set of rules that groups various different pixels in terms of their attributes that split the whole data into sub-categories. These categories are separated by decision boundaries which are then labelled according to the group [29].

By assigning labels according to these groups, users are able to obtain thematic maps [30]. As the name suggests, a thematic map is a type of map which focuses on a particular theme that is directly linked to a specific geographic region. Some examples of methods which could be used to classify a multi-spectral remote sensing product are:

- 1) Unsupervised classification
- 2) Supervised classification
- 3) Non-parametric statistics
- 4) Fuzzy classification
- 5) Crisp classification
- 6) Per-pixel classification
- 7) Object-based classification

[31].

J. Unsupervised classification

Unsupervised image classification is the process where each image in a given data-set is pointed out as a member of one of the fundamental categories which are present in the image collection without the need of using labelled training samples. The unsupervised grouping of images depend on unsupervised machine learning algorithms for its implementation [32]. Clustering used for unsupervised classification is one of most used methods for processing data from remote sensing data of the planet Earth [33].

III. ATMOSPHERIC CORRECTION

Atmospheric correction in remote-sensing is the removal of scattering and absorption effects coming from the atmosphere to obtain the surface properties. Prior reaching the sensor of the satellite, EM (Electro-Magnetic) radiation passes through the atmosphere twice. Irradiance is the downwelling (short-wave) radiation from the sun while radiance is the upwelling (long-wave) radiation from Earth to the sensor. Absorption however reduces the intensity with a haziness effect, making EM energy to scatter and redirects it in the atmosphere, leading to an adjacent effect where pixels close-by are shared⁸. This radiation-atmosphere interaction notably interferes with the multi-spectral sensors aboard remote-sensing satellites, especially data used for monitoring. As an example, land-use observations experience wave-length scattering as the radiation goes through the atmosphere [34]. Knowing this, [35] noted that it is the key to plan about potential impacts on the quality of the data. By knowing such interactions, appropriate atmospheric correction is applied during the pre-processing part of the satellite data. The sensor aboard the satellite records both the obvious reflected brightness coming from the object and also records the brightness of the atmosphere in tandem. This means that the value of any given pixel recorded is not the actual radiance reflecting from the object [36]. Hence the main point of atmospheric correction is to quantify both properties of the pixel value obtained. This is due to the fact that the value of each aspect catalogued by the sensor is not known. However, when the value of each property is recorded via atmospheric correction, the study can be done with the appropriate radiance values [35].

There are plenty of implementations of atmospheric correction [37], such as the Top of Atmosphere(TOA) correction, which is used in this study. These implementations are split into two types; Absolute and Relative correction methods [38]. The main difference between these methods is that the Absolute methods convert the Digital Number(DN) value to either surface reflection or surface radiance, while the Relative methods do not include the true reflectance due to the absence of a solid base of physics [39].

Furthermore, the absolute atmospheric correction implementations lessens the scattering and absorption process. This

⁸gisgeography.com/atmospheric-correction

happens due to gases and aerosols in the atmosphere. While the Relative implementations reduce the effects of the atmosphere and the effects of the directionality that happens on the surface. These effects of directionality result from the angle at which the sun is facing Earth. Hence, the Relative implementations decrease scatter and other effects [40].

As a side note, absolute methods are split into another two additional types. These are the absolute methods which rely on physics and transfer radiation and those Absolute methods which rely only on Images [39].

A. Analysis & Precision

One of the key parameters needed for the physical processes involving Earth's surface is LST [41]. Apart from being essential in temperature-related researches and studies, new methods and techniques for accurately determining LST has become vital for evaluating the exchange in energy and water with the atmosphere [42] for various research fields [43]–[45] such as Heat Waves [46]–[48], and most importantly for this research, Urban Heat Island in urban environments [49]–[53]

A study conducted by [54], looked into the precision of such Split-windows algorithm (SWA) methods using LandSat 8 and Sentinel 3 images in estimating the LST over the city of Granada in Spain. In this study, the choice of Sentinel-3 and LandSat 8 came down to the conclusion based on the relatively recent launch in orbit, since being the least in orbit means that their thermal bands are the least studied to date. Even though EcoStress has been launched in 2018, NASA did in fact warn of anomalies involving the primary storage unit, which has halted the ability of gathering scientific data for some time intervals. In order to determine the accuracy of these LST products, data was validated with the temperature values gathered from in situ, making use of high precision temperature and humidity probes. These probes were strategically placed around Grenada based on the different types of land cover established in the Corine Land Cover inventory (2020), these are:

- 1) Rural areas
- 2) Industrial areas
- 3) Suburban areas
- 4) Urban areas
- 5) Urban green areas

With the aid of statistical analysis, the correlation between the data obtained was determined, comparing the data source with seasonal and seasonal variations in the same city.

B. Detecting UHI

A study conducted in Crete, a Mediterranean island boasting a climate similar to the Maltese islands, investigated the UHI of a coastal town surrounded by the Aegean sea called Hania [55], accounting for 4,444.1 inhabitants/km² making it even more relevant to this study since Malta is also densely populated. From May 26, 2007 to October 24, 2007, temperature and relative humidity readings were taken using nine urban stations and three rural stations, totalling eight data loggers. Simultaneously, meteorological data for the town of

Hania was collected and elaborated, including wind speed and direction, barometric pressure, sunlight, and precipitation which were used for cross-correlation with the appearance of the urban heat island (UHI) phenomena [55]. As stated by this case study, the highest temperatures were observed inside the city as compared to the sub-urban areas. The relative humidity was also reported as being lowest in the city centre and highest along the coastlines. This demonstrates that there was a shortage of relative humidity throughout the city. The largest temperature difference happened on August 25, 2007, with an 8°C difference, while the smallest temperature difference occurred on July 31, 2007, with a 0.6°C difference. The total average temperature for the entire measurement was 2.6°C [55]. Furthermore, according to this case study, the intensity of UHI is at its highest towards the start of summer (i.e. June) and gradually declines after September. The largest temperature difference for this measurement occurred in July, presumably indicating that the UHI intensity is at its peak in regions with a Mediterranean climate during this month of the year.

Something interesting to note is that the Hania region is rather arid. It barely rains, but when it does, the impact of rainfall in this area is significant. Temperatures resulted in a significant drop in the severity of the UHI in the region [55]. As a result, one technique to alleviate the UHI is through precipitation.

In another research by [56], the city of Grenada was split into six different local climatic zones (LCZ): Compact vs Open High-Rise, Compact vs Open Low-Rise, Scattered Trees and Low Plants. This was done as an approach to characterise the landscape, making it possible to precisely identify the factors that have the most or least impact on each LCZ. In their research they also established a number of factors: Normalised Difference Vegetation Index (NDVI), Normalised Difference Built-Up (NDBI), Fraction Vegetation Cover (PV), Solar Radiation, Pollution, Impervious Surface Fraction Factor (ISA), Mean of Building Height Factor, Fraction of Building Facades, Number of Vehicles as a Factor, Wind, Altitude and Population Density. With these factors established, the correlation between the data gathered and the relationship between the independent and dependent variables of each LCZ was determined by using Panel Data method, a method of statistical analysis.

Using the strategy used in this research, [56] were able to represent the probable variances of each LCZ's conditions in the final results, making it a unique and strong approach. This is a particularly useful method for calculating UHI in a medium-sized city with strong thermal contrast and pollution (like Granada does), because it allows one to calculate both daytime and nighttime UHI based on the physical and environmental parameters of each LCZ.

Another research by [57], mentioned that there have been plenty of authors who have written about obtaining LST and urban heat islands on a spectral, temporal and spatial scale and the respective satellite sensors most suitable for SUHI (Surface Urban Heat Island) detection. But all of them focus on a

single city or urban agglomeration, where the definition for rural and urban areas was adapted for each study case which makes the job of comparison between cities around the world somewhat of a complication. So instead [57] proposed a new methodology on how to calculate and compare SUHI values generated from urban agglomerations internationally. Their method suggests calculating SUHI for three surrounding areas using only LST acquired during night-time. In their research, this method was applied to 71 selected urban agglomerations around the world.

IV. RESEARCH METHODOLOGY

The main objective of this research is to use remote sensing technology in order to study and observe UHI on the Maltese Island. Temperature and vegetation have long been studied using Normalised Difference Vegetation Index (NDVI), most of these studies even suggest that NDVI and LST complement each other and have an interrelationship [58]. Therefore, in order to study and observe UHI, this research will look at the level of vegetation and the land surface temperatures, as done by [59].

While remote sensing has come a long way since its inception, there are still some significant challenges to monitoring a small island in comparison to huge areas and characteristics seen elsewhere in the world. This problem might cause some issues when assessing in detail the Maltese landscape, since spatial resolution has always been the biggest challenge for the Maltese case study. However, this paper is very confident in being able to track and analyse the UHI effect in Malta, albeit with some challenging issues that other bigger study cases never have to experience. Since the recent Covid pandemic, the recent lockdown that the country experienced, could prove to hold some interesting data about how the UHI behaves and therefore shed more insights about understanding UHI in Malta. The main drawback of remote sensing is cloud coverage. This is not really an issue when studying the summer season, however it might prove challenging when observing the second quarter of the year. This research is expecting to find the UHI effect in Malta, especially in the most dense Urbanised areas. It is also expecting very high LST values and low NDVI values during Summer. On the contrary, since March, April, and May are considered wet months and therefore more vegetation is around the landscape, NDVI values are expected to be higher while LST to be much lower than Summer values. Since the Urban area is part of the coast line, lower than expected LST values are to be expected.

A. Collection of Data

Remote-sensing Satellites are a great tool for gathering and processing data related to LST. For this research, night-time remote-sensed products have been used, following the suggestions and observations of previously mentioned literature [19], [21], [60]. 74 SLSTR Level-2 LST products were gathered from the Sentinel-3 mission, available free on the Copernicus database over the months of March till August, from 2019

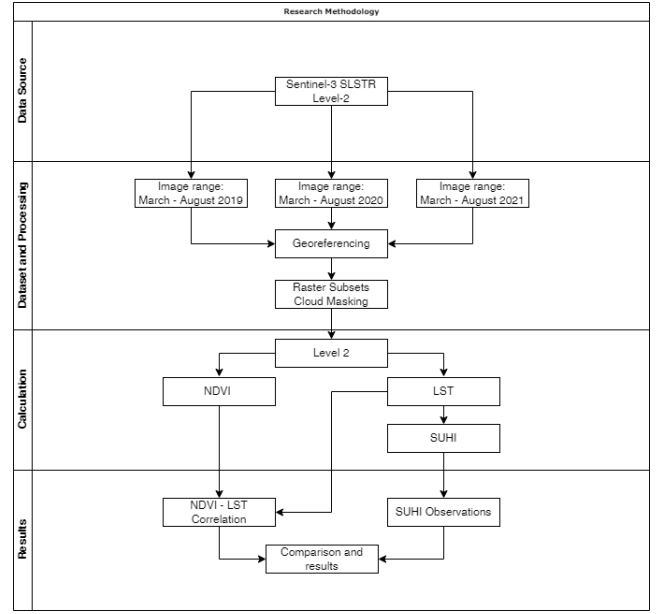


Fig. 1. Methodology used for this research.

up until 2021⁹. Apart from being able to produce both night-time and day-time products, Sentinel-3 also features an NDVI band which shall be used in conjunction with the LST values recorded. Most often, literature focuses on the extreme periods of the year such as the extreme heat of summer. However, given the recent events of the pandemic and its ensuing effects on society, for this research, the months of March till May will be used to observe UHI pre-pandemic, during pandemic and post-pandemic while using the months from June till August to better observe UHI and its growing presence on the Maltese Islands.

B. LST

The SLSTR Level-2 LST products that were used for this research feature land surface data generated on a 1km measurement grid which contains LST values that are computed and stored for each orphan or re-gridded pixel. Indexed across and along track dimensions are the Measurement Dataset (MD)¹⁰. This data set is processed using a split-window method, which use two different radiances from two channels. This is done to effectively determine the radiometric temperature of the Earth's surface. An algorithm is used for LST which is based on the radiative transfer theory which compare radiation between atmosphere and surface. This algorithm for LST can be stated as:

$$LST = a_0 + b_0 T_{11} + c_0 T_{12} \quad (1)$$

In this context; a_0 , b_0 and c_0 are coefficients which rely on land surface emissivity, atmospheric water vapour and satellite

⁹<https://scihub.copernicus.eu>

¹⁰<https://sentinels.copernicus.eu/web/sentinel/user-guides/sentinel-3-slstr/product-types/level-2-lst>

viewing angle. While T_{11} and T_{12} represents the brightness temperatures measured at 11 μm and 12 μm respectively¹¹.

C. NDVI

Most academic research regarding UHI involves the use of NDVI. NDVI or Normalised Difference Vegetation is used as an indicator of vegetation health present in a given area. Therefore, correlation between vegetation and LST can be calculated. NDVI data was taken from the NDVI band available directly from the data products provided by Copernicus. NDVI is calculated using the following formula:

$$NDVI = \frac{NIR - Red}{NIR + Red} \quad (2)$$

D. Study Area

The major hurdle in estimating $SUHI_{MEAN}$ and $SUHI_{MAX}$ is the difficulty in defining the urban area and its surrounding references since there is no clear definition in literature which explains how to select these areas [57].

The study area, consisting of the Maltese archipelago, was mapped using QGIS, an open-source geographic information application, which was used to assign geo-spatial vector data format. This was done by utilising the “New Shape File layer” function from QGIS, which exports the drawn polygon as a shapefile (.shp). This geo-spatial data is used to focus on specific areas, which shall be described later, of the previously downloaded data from the Copernicus database. Since the relative size of the islands and Eurostat describing Malta as being made up of two larger urban areas, “Valletta” and “Gozo”, it was decided that for this research, the main island of Malta would be split into two areas, the East side of Malta counting as the urban area while using the West of Malta as its rural area. Urban reference classification was sourced from the free land cover products produced by the European Space Agency Climate Change Initiative¹².

E. Preparing the Data

Prior manipulating the product for extracting and visualising data, each product had to be re-projected to the Coordinate Reference System (CRS) EPSG:4326 using ESA’s common architecture for all Sentinel Toolboxes, Snap Desktop. CRS is a coordinate-based global, regional or local system which is used to pinpoint geographical entities. CRS is used to define specific map projections while also allowing for transformations between two spatial reference systems. This allowed for the shape files created previously, to create data frames from the areas of interest while also being able to find the relevant pixel data according to location. Since the months of March and April result in mostly cloudy or rainy days, cloud masking had to be applied to the products. The basic idea of this approach is to detect clouds and cloud shadows by using the difference reflectance values between clear pixels and cloud

and cloud shadow contaminated pixels, therefore eliminating abnormal values from the final data set.

[61] describes the algorithm behind LST Uncertainty as a confront to the enormous challenge of using sensitive hardware from orbit, which as a minimum, distinguishes and quantifies between: locally correlated, large-scale systematic and random components should employ a consistent algorithm and a consistent approach to uncertainty analysis. Therefore for this study, any data that the algorithm flagged as having anything greater than 0.2 uncertainty. Cloud masking and the removal of 1st uncertainty of 0.2 was left out from the data set by setting an expression in the LST and NDVI band properties.

This was achieved by using the Snap Desktop built in “Batch Processing” feature and by running a graph consisting of a Read, Reproject, Subset and Write functions. By supplying the path location of the previously downloaded products, the Read function opens the products in their raw format. The reprojection function batch processed all of the products into EPSG:4326-WGS84. However, certain products which contained all of the data gathered in a single orbit, proved to take a considerable amount of time when reprojecting the image. Therefore, a Subset function was introduced which crops the image to a particular set of polygon coordinates. Although the Subset function was placed after the Reprojection function, it still functioned as intended and focused on reprojecting that subset rather than the whole orbit, thus reducing processing times. The Write function was used to convert the image produced from its original format into a GEOTIFF, which will be used later on in this research.

F. Spatial Mapping

SNAP consists of several toolboxes, some of which can be configured to work on Python by using the “Snappy” interface. By making use of snappy, large volumes of satellite data was efficiently analysed by automating the image processing tasks using python scripts. Metadata of each product, such as satellite name, date and time of recording was extracted and stored in the initial data frame, building an index of products and basic description. Each product was then split into multiple subsets using the previous shape files created for the study areas, focusing on the Maltese main island, the urban area and the rural area individually. Each subset is made up of two Raster bands LST and NDVI.

Null value for SLSTR Level-2 LST products is -32768. These values were removed, cleaning the data from the subsets. After cleaning the data values for LST and NDVI bands, new band data were created which were populated with pixel values and reshaped for each subset. Although not required, LST values were converted from the original Kelvin metric units to Celsius by subtracting 273.15 from their value. Values were normalised while mean, minimum and maximum pixel values were recorded for each subset. By using the libraries available from matplotlib, it was possible to generate a raster image from each subset. Both NDVI and LST raster interpolation was set to ‘nearest’, while the colour

¹¹<https://sentinels.copernicus.eu/web/sentinel/technical-guides/sentinel-3-s-lstr/level-2/lst-processing>

¹²<https://maps.elie.ucl.ac.be/CCI/viewer/>

maps for LST and NDVI were set to cm.jet and cm.RdYlGn respectively.

G. SUHI Surface Urban Heat Island

By following [57] methodology and using the night-time obtained LST, $SUHI_{MAX}$ and $SUHI_{MEAN}$, which can be described as thermal differences between the maximum and mean LST of the urban area and the LST surrounding area respectively, can be estimated by using this expression:

$$SUHI_{MAX} = LST_{URB-MAX} - LST_{SUR} \quad (3)$$

$$SUHI_{MEAN} = LST_{URB-MEAN} - LST_{SUR} \quad (4)$$

The definition for $LST_{URB-MAX}$ can be defined as the maximum LST (hottest pixel) of the urban area. $LST_{URB-MEAN}$ refers to the average temperature of the pixels defining the urban area, while LST_{SUR} can be described as the average temperature of the composing pixels in the surrounding area. Data recorded from the products were saved to a Comma Separated Values(CSV) file which shall be used for generating statistical data.

V. FINDINGS & DISCUSSION OF RESULTS

A. Data Validation

[62] concluded that for the three examined surfaces combined, the operational Sentinel-3A SLSTR LST product is accurate for nighttime data, with an accuracy (systematic uncertainty, i.e., median) of 1.0 K and a precision (random uncertainty, i.e., RSD) of 1.0 K. Therefore, since this research will focus on nighttime data, rigorous data validation will not be part of this chapter. However, for every product downloaded, weather station data has been logged, averaged and compared and referred to LST values throughout this chapter in order to better understand the results at hand.

B. Visualising and observing Data

For observation purposes, this section of this research will focus on the Maltese Islands overall, while observing for patterns or visual cues from the raster images and initial report produced prior extracting and analysing data. Data presented in this chapter consists of 74 products ranging from March till August 2019 - 2021. In depth detail about the data gathered will be tackled later on in this chapter.

The LST and NDVI heatmaps of the Maltese islands were obtained by following all the requisite steps as mentioned under the the Methodology, Chapter 3 of this research. This part focuses on the observations and analysis of the hotspots created by the UHI effect in Malta and how the towns and cities, mainly situated on the East side of Malta(island), affect the surrounding temperatures of the urban area by using the LST band from Sentinel-3 products. NDVI however shall be visualised solely for the purpose of observing, through out the given periods, how it correlates and affects LST values in the vicinity, its data is collected and used later on in the discussion of this research.

C. Observing LST

For the majority of the observations, when LST is compared to Land Cover data, it appears to be following the notion that the UHI effect, is a heat accumulation phenomenon often characterised by the urban climate created by urban constructions and general human activities [6], [7]. It can also be observed the quantity of thermal energy retention, mostly in urban areas, that dot the Maltese landscape, where green spaces and vegetative areas emit the least LST values while developed or barren areas emit the most, acknowledging the observations made by [15] that UHI comes from the decrease in vegetation, higher prevalence of dark surfaces and the increase in anthropogenic heat production.

The notion of Malta being composed of two larger urban areas, “Valletta” and “Gozo” by Eurostat, can be easily validated using the Land Cover data obtained from the European Space Agency Climate Change Initiative program. Therefore, this research assumes “Gozo” and “Valletta” as two separate Urban areas. When comparing “Gozo” with “Valletta”, the first remark that comes from observations is the density of the urban area and its affect on the surrounding area. “Gozo”, having somewhat minimal urbanisation in place, does not “pollute” and affect the surrounding areas as much as “Valletta”. This difference is mostly visible in the Summer period of the year, as peak LST could be seen taking place in areas which are in the surrounding areas of the urban area, with areas such as the south of Malta, where the Maltese Freeport international port station and the Delimara Power Station are located, show the extremities of human interference on a much wider area than usual.

Graph 2 displays Max LST and Mean LST for the island of Malta for the period of March till August from 2019 till 2021. At around the month of June each year, a noticeable spike in LST occurs. This observation can be linked to the fact that LST peaks during the beginning of summer (in June) and progressively drops after September. The largest temperature difference for this observation occurred in July, implying that the UHI intensity is at its highest in Mediterranean climate zones during this month [55].

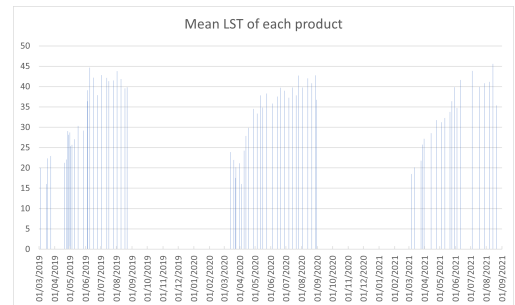


Fig. 2. Mean LST for each of the processed products in bar graph format

D. Observing NDVI

Temperature and vegetation have long been examined using the Normalised Difference Vegetation Index (NDVI), and

many of these research even show that NDVI and LST are complementary and have a link [58]. Therefore it was the obvious next step in this research to observe and analyse NDVI in relation to LST. By taking advantage of the NDVI band in Sentinel-3, NDVI readings compliment the LST values since they were recorded together on the same orbit. By using the same reprojected image produced for the LST band, an NDVI raster image is able to give out more details about the underlying contributors to the LST value recorded. NDVI values are set from 0, meaning barren and non-vegetative land, to 1, pointing out to lush vegetative green land. Therefore by comparing data from different periods, NDVI correlation can be observed and validated. The lack of vegetation on the Maltese Island throughout the majority of the year is an alarming observation, as the lack of green areas contribute to the accumulating rise in surface temperatures created by the UHI effect, hence the extreme LST values recorded in summer periods, which without plant transpiration and water evaporation from the soil, has no way of passively cooling the surrounding area.

E. Other Observations

Although vegetation and surface types are in fact the main contributors to high LST values, they are not the only driving force in play. As sometimes, LST values do not exactly follow the statements mentioned. [24] mentioned that the creation of the UHI is influenced by the climate and topography of cities, which are mostly governed by their geographical position and that the effect of the sea breeze on temperatures is mitigated by the presence of vast bodies of water. This phenomena overlaps with UHI in coastal cities, causing local climate change. Another study conducted in the city of Barcelona (Spain) found that the UHI intensity is weaker in the summer due to the sea breeze effect. As a result, the peak of UHI intensity occurs in December [63]. On the other hand, temperature inversions create stable atmospheric zones in the lower atmosphere, resulting in the trapping of pollutants near the ground surface. When the temperature rises with height, or when the potential temperature gradient is positive, this phenomena occurs. Situations like these arise as a result of the ground surface's radiative cooling which results in observing abnormal temperatures in regions or land areas which when following the conventional literature about inland cities says should not exist. Rainfall has a big impact on UHI. Temperatures in the region led in a dramatic reduction in the severity of the UHI, as mentioned in the research by [55].¹³

F. Analysing Data

In this section, this research will focus the study area to the island of Malta. By subsetting the previous image to focus on one island will give out clearer results as it will focus on just one urban area. As mentioned in the previous chapter, the study area will be further split into two parts; the Urban area and the Rural area. For the scope of this research, Urban

Area will be associated with the East of Malta, as there is the bulk of the high density urbanisation on the island, while the West shall be referred to as the Rural Area, accounting for the majority of the green spaces on the island. The data has been grouped and analysed into three-month periods, the "Summer" period and the "Covid" period. Part of this research will look for any abnormalities or deviancy in trend for the period accounting for the lockdown season experienced during the beginning of the pandemic, where most human activities came mostly to a sudden stop. Initial hypothesis stands to understand that some form of noticeable or observable data will come to fruition by studying the before, during and after this event. The "Summer" period however shall be used to analyse peak LST and for comparison between the two periods, as already been observed in the last section. The first part will focus the study area on the whole main island of Malta. In detail discussion of the urban area and rural area will be tackled in the second part of each period.

G. 2019 March - May

This period marks a year prior the lockdown season Maltese citizens experienced and as such, this data shall be used as a before human activities stopped briefly and how human activities affect UHI and LST without changing the landscape. Although 2019 is often referred to as the warmest year of a decade¹⁴, this period is marked as being the coldest period on average when compared to the rest of the periods. The lowest Minimum Average LST for the area of Malta recorded was on the 16th of March 2019, at 16.03°C, being the lowest Minimum LST value of the whole study periods. This is mostly attributed to the fact that it was recorded after a couple of weeks of heavy dew fall, light rain and thunderstorms. Max Average LST recorded for this period is also the lowest value recorded when compared to the other periods, at 30.3°C while LST median of the whole period is at 25.5°C. Mean LST for the period was at 24.9°C being also the lowest from the set of periods. Mean NDVI for the period is at the highest, with a mean value of 0.29, highest NDVI mean value recorded for the set.

Mean LST for the Rural area (West Malta) was at 24.4°C while the Urban area (East Malta) was at 25.3°C. A noticeable difference of 0.9°C between the two areas. Mean NDVI for the Urban Area was recorded at 0.27 while the Rural area was recorded at 0.32. $SUHI_{MEAN}$ for the period came out to be 0.97°C while $SUHI_{MAX}$ was at 4.6°C. Between 2nd May and 5th May 2019, rain and cloud coverage cooled down Mean LST for the urban area from 26.22°C to 25.76°C while the rural area increased in Mean LST from 24.18°C to 25.61. This could be the result of the sea breeze effect, which having the Urban area sitting on the coastline can benefit from. As already mentioned indirectly, this period was the hardest to track products which do not have clouds covering the study area. This is reflected in the low LST values recorded over this period, especially for the months of March and April

¹³<https://weatherspark.com/h/m/150260/2019/5/Historical-Weather-in-May-2019-in-Malta#Sections-Precipitation>

¹⁴<https://www.malteseislandsweather.com/category/reports/annual/>

while continuous clover cover and water precipitation may have contributed to the final analysis of this period. Overall, coldest recorded period and most vegetative with an above average $SUHI_{MAX}$ and $SUHI_{MEAN}$.

H. 2019 June - August

This period marks the earliest record of this study towards analysing the extreme temperatures which happen in Summer. Since Summer 2020 was not part of that lockdown season, this period will not be included with the Covid analysis. Summer 2019 marks the period with the lowest average LST of 36.37°C, recorded on the 4th of June 2019. Understandably, the lowest average recorded is at the earliest of the period with temperatures plateauing at the beginning of August, marking a reversal in trend which sees the rest of the month with decreasing LST values. However, the highest Max LST of this period was in early June, where it peaked at 50.2°C, results conform with the statement that LST peaks during the beginning of summer, around June, and progressively drops after September [55]. NDVI values for this period is at a slow steady decline starting at NDVI value 0.25 at the beginning of June and ends the period with a value of 0.21°C, signalling dry season for the most part of the period.

Mean LST for the Rural Area was at 40.6°C, while that of the Urban area was 41.9°C, with a difference of 1.3°C it is slightly higher than the difference collected between March and May of 2019. $SUHI_{MAX}$ was at 5°C while $SUHI_{MEAN}$ was recorded as 1.3°C. SUHI values for this period were the lowest from the study periods. This could be due to the fact that although $SUHI_{MAX}$ and $SUHI_{MEAN}$ were indeed a little lower than usual throughout this period, it was also one of the most stable out of the whole study periods and therefore would not impact the averaged result as much. Mean NDVI levels were both below average when compared to the other periods, with the Urban area having an NDVI value of 0.2 while the Rural area averaged 0.24.

I. 2020 March - May

This period marks the year when the lockdown restrictions took place in Malta for the majority of the time frame¹⁵. This means that for a brief moment in history, human activities have halted to running only the essentials, making this an opportunity to study and observe. Although UHI itself is not dependent on ongoing activities, it is still an important contributor which might give some new insights on the subject. Minimum Averaged LST was 16.05°C while the Max LST recorded was 44.58°C. This contrast in extreme LST values when compared to the previous year could be attributed to less rainfall during this period when compared to previous years¹⁷. On the 23rd and 24th of March 2020, NDVI values recorded

had a sudden downward spike and then returns to normal values. Upon further investigation, this turned out to be cloud coverage over Malta and the low NDVI reflected as a result of the cloud masking, which nulls the pixel data where clouds are detected. However, Mean NDVI value was 0.26, which is equal to the average Mean NDVI value of all “Covid” periods. Average $SUHI_{MAX}$ was at 4.6°C while $SUHI_{MEAN}$ was recorded as 0.64°C, a decrease from the previous year. This could be attributed to the unnaturally drier season than usual.

J. 2020 June - August

During this period, lockdown restrictions were mostly eased or in the works of phasing out. Therefore this period will not be included with the “Covid” period. Minimum average LST and Max averaged LST both were recorded to be cooler than the previous year, with a 35.85°C Minimum LST and a 47°C for Max LST. This makes this years lowest recorded LST by around 0.5°C and a cooler Max LST value difference of 3.2°C than the previous year. Mean LST was at 39.4°C, making it cooler than the previous year.

Mean LST over the Rural area was 1.1°C cooler than the Urban area, with values recorded being 39°C for the Rural area and 40.1°C of the Urban area. Mean NDVI showed was as expected, that is NDVI between Rural and Urban areas in summer due to the dryness of the season, difference between the areas is at a minimal. With the Urban area having a mean NDVI value of 0.19 while the Rural area had a 0.22. Average $SUHI_{MAX}$ was at 4.9°C while $SUHI_{MEAN}$ was 1.2°C.

K. 2021 March - May

This period marks a year from the lockdown restrictions. Mean LST for the period was at 28.5°C while Max LST recorded was 47°C, making them the highest average LST value and Max LST recorded value for the “Covid” group. This could be due to the fact that the year 2021 was warmer than usual. The yearly average was exceeded by 1.6 degrees Celsius, with a mean temperature of 19.8 degrees Celsius. Maximum temperatures showed the biggest deviation from the climatic mean. Only the months of March, April, October, and December had temperatures below the average. Over the course of the year, a number of temperature-related records were broken. On the second weekend of 2021, on Saturday, January 9th, Malta set a new national record for the highest January temperature ever recorded¹⁸. These are alarming events where the whole climate can be seen to be getting warmer and drier sooner each passing year. However, Mean NDVI value was still at 0.26, the same as the previous year.

Average Mean LST over this period for the Rural Area was at 28°C while the Urban Area had a slightly higher average of 29.3°C, the highest from the “Covid” period group. NDVI values in the Urban area showed at 0.24 while in the Rural area it was averaged at 0.28. Average $SUHI_{MAX}$ was at 4.4°C while $SUHI_{MEAN}$ was 1.23°C.

¹⁵<https://www.mondaq.com/human-rights/912314/partial-lockdown-in-malta-to-have-effect-from-28-march-2020>

¹⁶https://www.maltatoday.com.mt/news/national/108479/how_covid_experts_postlockdown_plan_called_for_travel_ban_until_september_2020#.YpThQKhBwuU

¹⁷<https://www.malteseislandsweather.com/category/reports/annual/>

¹⁸<https://www.malteseislandsweather.com/category/reports/annual/>

L. 2021 June - August

This is the final period for this study to analyse. The average Mean LST for this period was at 40.4°C while Max LST was 50.1°C, which is noticeably higher than the previous years. Average Mean NDVI was recorded at 0.19, well within average. Mean LST for the Urban Area was 40.9 while in the Rural area it was at 40.1°C. NDVI value for the Rural area was at 0.2 while the urban area was recorded at 0.18. $SUHI_{MEAN}$ for the period was 0.75°C while $SUHI_{MAX}$ was at 4.9°C.

M. Overall Analysis

This part of the research will focus on the overall results gathered alongside the observations done in the beginning of this chapter. The study periods that will be mentioned are the “Covid” and “Summer” periods. Results are compared and analysed in detail individually depending on the period being discussed.

N. 2019 March - May — 2021 March - May

Overall, for the “Covid” period, an upward trend in LST values and a downward trend for NDVI was observed. Mean LST increased by 15% going from an averaged LST of 24.86°C in 2019 to 28.53°C in 2021. An interesting point about the study areas is that this increase in temperature is shared equally between the Rural and Urban areas. This means that the Rural area was not able to dissipate heat any quicker than the Urban area. Mean NDVI saw a decrease of 12.4% from 2019 till 2021. However, the decrease in NDVI values in the Rural areas were higher than the Urban Area, with a 13% decrease in the Rural area compared to the 10% decrease in the Urban area. $SUHI_{MAX}$ saw a decrease of 5% while $SUHI_{MEAN}$ increased by 26.6%. An interesting point about this period is that a slight decrease in uptrend was noticed throughout the year 2020. This means that daily human activities, although not enough to reverse the uptrend immediately, are also part of the bigger picture when studying UHI.

O. 2019 June - August — 2021 June - August

For the “Summer” period however, it was the opposite of the “Covid” period. This time frame saw a decrease in Mean LST of 1.5%. Interestingly, mean LST experienced a drop in temperature between Summer 2019 and 2020, as it decreased from 41°C to 39.4°C in 2020. Then in Summer of 2021, temperatures reach almost 2019 levels, at 40.4°C. This downward trend was equal as well between the Rural and Urban areas, having experienced a decrease of 1% and 2% respectively. Mean NDVI however did not see any signs of reversal, as it decreased by 11.4% between 2019 and 2021 and saw no significant changes in the downtrend as visible with LST. Rural areas suffered the most, with a decrease in Mean NDVI of 18.5% decrease compared to the Urban Area’s 14.7% decrease. This downtrend in NDVI could be explained by the increasing development the island is experiencing. Between Spring 2017 and Spring 2019, the vegetation green colour

on the islands decreased by 2.45km². This loss could be the result of tree chopping, fewer vegetation, and reduced farming activity while over the course of four years, the Islands’ arable and rural areas were degraded by 1.25km², with 0.83km² eroded in the past two years. This loss is due to a variety of factors, including increased urbanization and the expansion of urban zones [64]. $SUHI_{MAX}$ saw a decrease of 2.5% while $SUHI_{MEAN}$ somewhat experienced a decrease of 41% from 2019 till 2021. Having decreased from 1.27 to 1.15 between 2019 and 2020, while 2021 came as a surprisingly lower value of 0.75. This value could be result of an anomaly in the data collected on the 21st of August 2021 when $SUHI_{MEAN}$ was recorded at -1.68 due to a sudden decrease in temperatures between the 14th and the 21st of August, 2021.

P. LST vs NDVI correlation

Part of this research includes the exploration of the correlation between LST and NDVI. With the data gathered from all the products, results are as follow; Correlation Coefficient of the main island of Malta is at -0.54, the correlation coefficient of the Rural Area was -0.58 while correlation coefficient of the Urban Area was -0.48, see Figure 3. This discrepancy between the Urban and Rural area raise the issue that although LST and NDVI are clearly correlated, there are other factors implicating the effects of NDVI on LST. The most obvious of these factors is the density of water bodies nearby or the water retention available in the air in the form of humidity or dew. Not to mention the inclusion of NDVI and topography of the study area as observed in the beginning of this chapter and mentioned in other literature [24], [55], [63].

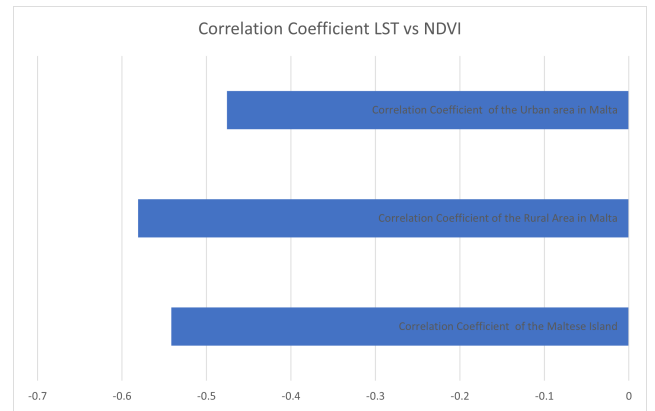


Fig. 3. A bar graph displaying the correlation coefficient between Mean LST and Mean NDVI all periods studied

VI. CONCLUSION

A. Overview

The major goal of this study was to examine and observe UHI on the Maltese island using remote sensing technology. The Normalised Difference Vegetation Index (NDVI) has long been used to study temperature and vegetation; in fact, most of the research implies that NDVI and LST complement each other and have a relationship [58]. As a result, in order to

analyse and detect UHI, this study looked at vegetation levels and land surface temperatures, as done by [59]. From March to August, from 2019 to 2021, 74 SLSTR Level-2 LST night-time products were obtained from the Sentinel-3 mission, freely available on the Copernicus database. These products served as a model for evaluating mean LST values over a period of time. Sentinel-3 has an NDVI band that was used in conjunction with the LST values recorded. Given the recent events of the pandemic and their societal implications, the months of March to May were used to watch UHI during pre-pandemic, during the pandemic, and after the pandemic. Meanwhile the months of June to August were utilised to better observe UHI and its rising presence on the Maltese Islands.

The free land cover products supplied by the European Space Agency Climate Change Initiative were used as a basis for the urban reference categorisation. By using the land cover data as reference, the Maltese archipelago was mapped using QGIS, an open-source geographic information program that was used to assign geo-spatial vector data format. Due to the relative size of the islands, reference land cover data from ESA and Eurostat's description of Malta as being made up of two larger urban areas, "Valletta" and "Gozo", it was decided that the main island of Malta would be divided into two areas for this study, with the East side of Malta counting as the urban area and the West as the rural area.

Each product downloaded had to be re-projected to the Coordinate Reference System (CRS) EPSG:4326 using ESA's common architecture, Snap Desktop. This allowed the previously prepared shape files to create data frames from the areas of interest while also allowing the relevant pixel data to be found based on location. Cloud masking had to be applied to the products because the months of March and April are generally cloudy or wet.

Large amounts of satellite data were efficiently analysed utilising snappy by automating image processing activities with python scripts. The previous shape files developed for the research areas were then used to partition each product into different subsets, focusing on the Maltese main island, the urban area, and the rural area separately. By using [57]'s methodology and making use of the night-time obtained LST, $SUHI_{MAX}$ and $SUHI_{MEAN}$, which can be described as thermal differences between the maximum and mean LST of the urban area and the LST surrounding area respectively, were used in order to better understand, track and observe the UHI effect. For the observation part, UHI does indeed exist in Malta. It can also be seen how much thermal energy is retained in the Maltese landscape, with green spaces and vegetative areas emitting the least LST values and developed or barren areas emitting the most, confirming [15]'s findings that UHI is caused by a decrease in vegetation, a higher prevalence of dark surfaces, and an increase in anthropogenic heat production. Peak LST could be seen in areas near urban areas, with areas such as the south of Malta, where the Maltese Freeport international port station and the Delimara Power Station are located, showing the extremes of human influence over a considerably larger area than what is typically expected.

Considering the fact that Malta has double the sunshine hours of other cities Northern Europe, these high LST values are to be expected, especially for the summer season when Malta averages 12 hours of continuous sunshine (July).

Overall, for the "Covid" period, an upward trend in LST values and a downward trend for NDVI was observed. Mean LST increased by 15% going from an averaged LST of 24.86°C in 2019 to 28.53°C in 2021. An interesting point about this period is that the increase in temperature was shared equally between the Rural and Urban areas. This means that the Rural area was not able to dissipate heat any quicker than the Urban area. A fascinating aspect of this time period is that the uptrend slowed slightly throughout the year 2020. This means that, while daily human activities aren't enough to immediately reverse the upward trend, they are part of the larger picture when studying UHI.

The "Summer" period, on the other hand, was the polar opposite of the "Covid" period. The Mean LST fell by 1.5% during this time period. Intriguingly, the mean LST decreased from 41°C in Summer 2019 to 39.4°C in Summer 2020. Then, in the summer of 2021, temperatures reach 40.4°C, nearly matching those of 2019.

The correlation between LST and NDVI was also investigated as part of this study. As previously discussed, LST and NDVI have been observed as having some type of correlation. By using all the products downloaded as a base and using the Mean LST and the Mean NDVI, a correlation pattern was confirmed. The main island of Malta was found of having a correlation coefficient of -0.54, the Rural Area has a correlation coefficient of -0.58, and the Urban Area has a correlation coefficient of -0.48. This disparity between the urban and rural areas raises the possibility that, while LST and NDVI are clearly correlated, other factors may be influencing NDVI's effects on LST. The density of nearby water bodies or the water retention available in the air in the form of humidity or dew are the most obvious of these factors. Not to mention the inclusion of NDVI and topography of the study area, as mentioned in the previous chapter and in literature reviewed [24], [55], [63].

B. Limitations and Recommendations

The idea of using a single remote sensing data source came with its disadvantages. The theory behind it was that by using a single data set, this research would avoid to go into exploring how varying ratings of inaccuracies between different satellites, would affect the final results. However, the inclusion of other satellites would be of greater importance as it would add more contextual data about the study area such as information on topography such as the Operational Land Imager (OLI) and Thermal Infrared Sensor (TIR) in LANDSAT 8 and the Enhanced Thematic Mapper (ETM+) in LANDSAT 7. With a greater arsenal of metrics, analysing and observing UHI would lead to a better understanding of the phenomena.

The use of land cover reference in this research could have been done in better detail. Instead of using the data as a

visual reference and plotting manually the study areas, another recommendation would be to use the actual pixel values from the the land cover data and compare it with the relevant LST pixel value. A much more detailed perspective of this research would be possible with this method. On top of that, adding the inclusion of sun hours in correlation with LST or even vegetation height in coupled with NDVI could lead for more elaborate findings.

Whilst conducting this research it was noticed that apart from the obvious cloud coverage limitation that plague remote sensing satellites, Sentinel-3 had other issues. These issues came in the form of malfunctions and maintenance. Being an expensive probe, orbiting the Earth exposed to radiation, malfunctions are to be expected. Coupled with the fact that during winter, cloud coverage is almost constant, having a malfunction or maintenance schedule could be the difference between finding a product with cloud coverage or without. Therefore, during winter time, it is advisable to make use of local weather and data stations to track and monitor UHI in Malta. However, that does not make the summer period irrelevant, as this study proved by observing the extremities of the summer heat.

Processing multi-spectral images, although minimum requirements are not high, can draw an immense load on the processing machine. Full-orbital images hit the machine worst, as a single processed image would amass around 30GB of data. Obviously to process that amount of data requires a great deal of processing power. As mentioned in this study methodology, a work around for this was to focus the reprojection process on the subset created in the initial phase of processing the data. Therefore investing in better equipment such as faster data storage, bigger memory and a more efficient processor would certainly make the analysis of greater time periods possible. An alternative would be exploring the possibilities that a Kubernetes system would achieve.

The location of the Sun in the sky may have influenced the final result's accuracy. This is due to the fact that the Earth's location on the Sun's orbital plane is always changing, therefore, the Sun's position in the sky fluctuates with the changing seasons [65]. This orbital shift impacts what is reflected back to the satellites' sensors, as well as the degree of shadowing on the ground, impacting the overall accuracy of the results [66].

REFERENCES

- [1] M. Pacione, *U Ban Geography: A Global Perspective*. Routledge, 2009.
- [2] T. J. Nechyba and R. P. Walsh, "Urban sprawl," *Journal of Economic Perspectives*, vol. 18, no. 4, pp. 177–200, 2004.
- [3] B. Bhatta, S. Saraswati, and D. Bandyopadhyay, "Urban sprawl measurement from remote sensing data," *Applied Geography*, vol. 30, no. 4, pp. 731–740, 2010, climate Change and Applied Geography – Place, Policy, and Practice. [Online]. Available: <https://www.sciencedirect.com/science/article/pii/S0143622810000226>
- [4] M. Melchiorri, A. J. Florczyk, S. Freire, M. Schiavina, M. Pesaresi, and T. Kemper, "Unveiling 25 years of planetary urbanization with remote sensing: Perspectives from the global human settlement layer," *Remote Sensing*, vol. 10, no. 5, p. 768, 2018.
- [5] K. C. Tan, H. S. Lim, M. Z. Mat Jafri, and K. Abdullah, "Landsat data to evaluate urban expansion and determine land use/land cover changes in penang island, malaysia," *Environmental Earth Sciences*, vol. 60, pp. 1509–1521, 06 2009.
- [6] A. J. Arnfield, "Two decades of urban climate research: a review of turbulence, exchanges of energy and water, and the urban heat island," *International journal of climatology*, vol. 23, pp. 1–26, 2003.
- [7] T. Nakayama and T. Fujita, "Cooling effect of water-holding pavements made of new materials on water and heat budgets in urban areas," *Landscape and Urban Planning*, vol. 96, no. 2, pp. 57–67, 2010. [Online]. Available: <https://www.sciencedirect.com/science/article/pii/S0169204610000344>
- [8] T. R. Oke, "The energetic basis of the urban heat island," *Quarterly Journal of the Royal Meteorological Society*, vol. 108, no. 455, pp. 1–24, 1982.
- [9] L. Yang, F. Qiana, D.-X. Song, and K.-J. Zheng, "Research on urban heat-island effect," *Procedia Engineering*, pp. 11–18, 2016.
- [10] H. Landsberg, in *The Urban Climate*. New York, NY, USA: Academic Press, 1981.
- [11] T. R. Karl, H. F. Diaz, and G. Kukla, "Urbanization: Its detection and effect in the united states climate record," *Journal of Climate*, vol. 1, pp. 1099–1123, 1988.
- [12] P. Torrens, "A toolkit for measuring sprawl," *Applied Spatial Analysis and Policy*, vol. 1, pp. 5–36, 04 2008.
- [13] G. Galster, R. Hanson, M. Ratcliffe, H. Wolman, S. Coleman, and J. Freihage, "Wrestling sprawl to the ground: Defining and measuring an elusive concept," *Housing Policy Debate*, vol. 12, pp. 681–717, 01 2001.
- [14] M. Santamouris, *Energy and climate in the urban built environment*. Routledge, 2013.
- [15] B. Stone, J. J. Hess, and H. Frumkin, "Urban form and extreme heat events: Are sprawling cities more vulnerable to climate change than compact cities?" *Environmental Health Perspectives*, vol. 118, no. 10, p. 1425–1428, 2010.
- [16] H. Akbari and L. S. Rose, "Urban surfaces and heat island mitigation potentials," *Journal of the Human-Environment System*, vol. 11, no. 2, pp. 85–101, 2008.
- [17] M. Roth, T. R. Oke, and W. J. Emery, "Satellite-derived urban heat islands from three coastal cities and the utilization of such data in urban climatology," *International Journal of Remote Sensing*, vol. 10, pp. 1699–1720, 1989.
- [18] T. N. Carlson, J. K. Dodd, S. G. Benjamin, and J. N. Cooper, "Satellite estimation of the surface energy balance, moisture availability and thermal inertia," *Journal of Applied Meteorology*, vol. 20, pp. 67–87, 1981.
- [19] C. B. Karakuş, "The impact of land use/land cover (lulc) changes on land surface temperature in sivas city center and its surroundings and assessment of urban heat island," *Asia-Pacific Journal of Atmospheric Sciences volume*, vol. 55, pp. 669–684, 2019.
- [20] C. Yang, R. Wang, S. Zhang, C. Ji, and X. Fu, "Characterizing the hourly variation of urban heat islands in a snowy climate city during summer," *International Journal of Environmental Research and Public Health*, vol. 16, no. 14, 2019. [Online]. Available: <https://www.mdpi.com/1660-4601/16/14/2467>
- [21] C. Yang, F. Yan, and S. Zhang, "Comparison of land surface and air temperatures for quantifying summer and winter urban heat island in a snow climate city," *Journal of Environmental Management*, vol. 265, p. 110563, 2020. [Online]. Available: <https://www.sciencedirect.com/science/article/pii/S0301479720304965>
- [22] CaiyanWu, J. Li, C. Wang, C. Song, Y. Chen, M. Finka, and D. L. Rosa, "Understanding the relationship between urban blue infrastructure and land surface temperature," *Science of The Total Environment*, vol. 694, 2019.
- [23] M. Lemus-Canovas, J. Martin-Vide, M. C. Moreno-Garcia, and J. A. Lopez-Bustins, "Estimating barcelona's metropolitan daytime hot and cold poles using landsat-8 land surface temperature," *Science of The Total Environment*, vol. 699, p. 134307, 2020. [Online]. Available: <https://www.sciencedirect.com/science/article/pii/S0048969719342962>
- [24] A. Martinelli, D.-D. Kolokotsa, and F. Fiorito, "Urban heat island in mediterranean coastal cities: The case of bari (italy)," *Climate*, vol. 8, no. 6, p. 79, 2020.
- [25] A. S. Nouri, J. P. Costa, and A. Matzarakis, "Examining default urban-aspect-ratios and sky-view-factors to identify priorities for thermal-sensitive public space design in hot-summer mediterranean climates:

- The lisbon case,” *Building and Environment*, vol. 126, pp. 442–456, 2017.
- [26] I. D. Stewart, T. R. Oke, and E. S. Krayenhoff, “Evaluation of the ‘local climate zone’ scheme using temperature observations and model simulations,” *International journal of climatology*, vol. 34, no. 4, pp. 1062–1080, 2014.
 - [27] C. Cardelino and W. Chameides, “Natural hydrocarbons, urbanization, and urban ozone,” *Journal of Geophysical Research*, vol. 95, pp. 13,971–13,979, 1990.
 - [28] B. Stone Jr and M. O. Rodgers, “Urban form and thermal efficiency: how the design of cities influences the urban heat island effect,” *American Planning Association. Journal of the American Planning Association*, vol. 67, no. 2, p. 186, 2001.
 - [29] C. Elachi and J. J. Van Zyl, *Introduction to the physics and techniques of remote sensing*. John Wiley & Sons, 2021.
 - [30] R. Schowengerdt, “Thematic classification,” *Remote Sensing: Models and Methods for Image Processing. 2nd ed. San Diego, CA: Academic*, pp. 457–451, 1997.
 - [31] J. R. Jensen, “Introductory digital image processing: a remote sensing perspective,” Univ. of South Carolina, Columbus, Tech. Rep., 1986.
 - [32] A. Olade, G. Naghdy, and C. Todd, “Unsupervised classification of images: A review,” *International Journal of Image Processing*, vol. 8, pp. 2014–325, 09 2014.
 - [33] J. Jensen, “Introductory digital image processing: A remote sensing perspective,” *Prentice Hall, Inc.*, pp. 197–256, 1996.
 - [34] F. Bian, D. Fan, Y. Zhang, and D. Wang, “Synchronous atmospheric radiation correction of gf - 2 satellite multispectral image.” p. 10697, 2018.
 - [35] D. G. Hadjimitsis, G. Papadavid, A. Agapiou, K. Themistocleous, M. Hadjimitsis, A. Retalis, S. Michaelides, N. Chrysoulakis, L. Toullos, and C. Clayton, “Atmospheric correction for satellite remotely sensed data intended for agricultural applications: impact on vegetation indices,” *Natural Hazards and Earth System Sciences*, vol. 10, no. 1, pp. 89–95, 2010.
 - [36] P. Tyagi and U. Bhosle, “Radiometric correction of multispectral images using radon transform,” *Journal of the Indian Society of Remote Sensing*, vol. 42, no. 1, pp. 23–34, 2014.
 - [37] C. O. Ilori, N. Pahlevan, and A. Knudby, “Analyzing performances of different atmospheric correction techniques for landsat 8: application for coastal remote sensing,” *Remote Sensing*, vol. 11, no. 4, p. 469, 2019.
 - [38] A. S. Mahiny and B. J. Turner, “A comparison of four common atmospheric correction methods,” *Photogrammetric Engineering & Remote Sensing*, vol. 73, no. 4, pp. 361–368, 2007.
 - [39] X. Yu, Q. Yan, and Z. Liu, “Atmospheric correction of hj-1a multi-spectral and hyper-spectral images,” in *2010 3rd International Congress on Image and Signal Processing*, vol. 5. IEEE, 2010, pp. 2125–2129.
 - [40] V. Caselles and M. Lopez Garcia, “An alternative simple approach to estimate atmospheric correction in multitemporal studies,” *International Journal of Remote Sensing*, vol. 10, no. 6, pp. 1127–1134, 1989.
 - [41] W. Zhan, Y. Chen, J. Zhou, J. Wang, W. Liu, J. Voogt, X. Zhu, J. Quan, and J. Li, “Disaggregation of remotely sensed land surface temperature: Literature survey, taxonomy, issues, and caveats,” *Remote Sensing of Environment*, vol. 131, pp. 119–139, 2013.
 - [42] X. Yu, X. Guo, and Z. Wu, “Land surface temperature retrieval from landsat 8 tirs—comparison between radiative transfer equation-based method, split window algorithm and single channel method,” *Remote sensing*, vol. 6, no. 10, pp. 9829–9852, 2014.
 - [43] J. Cheng, S. Liang, J. Wang, and X. Li, “A stepwise refining algorithm of temperature and emissivity separation for hyperspectral thermal infrared data,” *IEEE Transactions on Geoscience and Remote Sensing*, vol. 48, no. 3, pp. 1588–1597, 2009.
 - [44] E. Valor and V. Caselles, “Mapping land surface emissivity from ndvi: Application to european, african, and south american areas,” *Remote sensing of Environment*, vol. 57, no. 3, pp. 167–184, 1996.
 - [45] Z. Wan and J. Dozier, “A generalized split-window algorithm for retrieving land-surface temperature from space,” *IEEE Transactions on geoscience and remote sensing*, vol. 34, no. 4, pp. 892–905, 1996.
 - [46] S. Jiang, X. Lee, J. Wang, and K. Wang, “Amplified urban heat islands during heat wave periods,” *Journal of Geophysical Research: Atmospheres*, vol. 124, no. 14, pp. 7797–7812, 2019.
 - [47] D. Li and E. Bou-Zeid, “Synergistic interactions between urban heat islands and heat waves: The impact in cities is larger than the sum of its parts,” *Journal of Applied Meteorology and Climatology*, vol. 52, no. 9, pp. 2051–2064, 2013.
 - [48] P. Ramamurthy and E. Bou-Zeid, “Heatwaves and urban heat islands: a comparative analysis of multiple cities,” *Journal of Geophysical Research: Atmospheres*, vol. 122, no. 1, pp. 168–178, 2017.
 - [49] T. Barbieri, F. Despini, and S. Teggi, “A multi-temporal analyses of land surface temperature using landsat-8 data and open source software: The case study of modena, italy,” *Sustainability*, vol. 10, no. 5, p. 1678, 2018.
 - [50] C. Keeratikasikorn and S. Bonafoni, “Urban heat island analysis over the land use zoning plan of bangkok by means of landsat 8 imagery,” *Remote Sensing*, vol. 10, no. 3, p. 440, 2018.
 - [51] A. Khalaf, “Utilization of thermal bands of landsat 8 data and geographic information system for analysis of urban heat island in baghdad governorate 2016,” in *MATEC Web of Conferences*, vol. 162. EDP Sciences, 2018, p. 03026.
 - [52] P. Macarof and F. Statescu, “Comparasion of ndbi and ndvi as indicators of surface urban heat island effect in landsat 8 imagery: a case study of iasi,” *Present Environment and Sustainable Development*, no. 2, pp. 141–150, 2017.
 - [53] A. Sekertekin, “Validation of physical radiative transfer equation-based land surface temperature using landsat 8 satellite imagery and surfrad in-situ measurements,” *Journal of Atmospheric and Solar-Terrestrial Physics*, vol. 196, p. 105161, 2019.
 - [54] D. Hidalgo García, “Analysis and precision of the terrestrial surface temperature using landsat 8 and sentinel 3 images: Study applied to the city of granada (spain),” *Sustainable Cities and Society*, vol. 71, p. 102980, 2021. [Online]. Available: <https://www.sciencedirect.com/science/article/pii/S2210670721002663>
 - [55] D. Kolokotsa, A. Psomas, and E. Karapidakis, “Urban heat island in southern europe: The case study of hania, crete,” *Solar Energy*, vol. 83, no. 10, pp. 1871–1883, 2009.
 - [56] D. Hidalgo García and J. Arco Díaz, “Modeling of the urban heat island on local climatic zones of a city using sentinel 3 images: Urban determining factors,” *Urban Climate*, vol. 37, p. 100840, 2021. [Online]. Available: <https://www.sciencedirect.com/science/article/pii/S2212095521000705>
 - [57] J. A. Sobrino and I. Irakulis, “A methodology for comparing the surface urban heat island in selected urban agglomerations around the world from sentinel-3 slstr data,” *Remote Sensing*, vol. 12, no. 12, p. 2052, 2020.
 - [58] Z. Guo, S. Wang, M. Cheng, and Y. Shu, “Assess the effect of different degrees of urbanization on land surface temperature using remote sensing images,” *Procedia Environmental Sciences*, vol. 13, pp. 935–942, 2012.
 - [59] D. H. García, “Analysis of urban heat island and heat waves using sentinel-3 images: a study of andalusian cities in spain,” *Earth Syst Environ*, 2021.
 - [60] Y. Hu, Z. Dai, and J.-M. Guldmann, “Modeling the impact of 2d/3d urban indicators on the urban heat island over different seasons: A boosted regression tree approach,” *Journal of Environmental Management*, vol. 266, p. 110424, 2020.
 - [61] D. Ghent, K. Veal, T. Trent, E. Dodd, H. Sembhi, and J. Remedios, “A new approach to defining uncertainties for modis land surface temperature,” *Remote Sensing*, vol. 11, no. 9, p. 1021, 2019.
 - [62] L. Pérez-Planells, R. Niclòs, J. Puchades, C. Coll, F.-M. Götsche, J. A. Valiente, E. Valor, and J. M. Galve, “Validation of sentinel-3 slstr land surface temperature retrieved by the operational product and comparison with explicitly emissivity-dependent algorithms,” *Remote Sensing*, vol. 13, no. 11, p. 2228, 2021.
 - [63] A. Salvati, H. C. Roura, and C. Cecere, “Assessing the urban heat island and its energy impact on residential buildings in mediterranean climate: Barcelona case study,” *Energy and Buildings*, vol. 146, pp. 38–54, 2017.
 - [64] S. Zerafa, “Measuring the loss of arable and rural lands on the maltese islands through satellite images,” 07 2020.
 - [65] W. Tang, K.-L. Ou, Y.-C. Lu, Y.-S. Shih, and H.-H. Liou, “A sun path observation system based on augment reality and mobile learning,” *Mobile Information Systems*, vol. 2018, 2018.
 - [66] X. Ma, A. Huete, N. N. Tran, J. Bi, S. Gao, and Y. Zeng, “Sun-angle effects on remote-sensing phenology observed and modelled using himawari-8,” *Remote Sensing*, vol. 12, no. 8, p. 1339, 2020.